Phase properties of the cutoff high-order harmonics

M. A. Khokhlova[1,2,*] and V. V. Strelkov[1,3]

[1]*A.M. Prokhorov General Physics Institute of the RAS, Moscow 119991, Russia*

[2]*Faculty of Physics, M.V. Lomonosov Moscow State University, Moscow 119991, Russia*

[3]*Moscow Institute of Physics and Technology (State University), 141700 Dolgoprudny, Moscow Region, Russia*

(Received 21 October 2015; published 20 April 2016)

The cutoff regime of high-order harmonic generation (HHG) by atoms in an intense laser field is studied numerically and analytically. We find that the cutoff regime is characterized by equal dephasing between the successive harmonics. The change of the harmonic phase locking when HHG evolves from the cutoff to the plateau regime determines the optimal bandwidth of the spectral region which should be used for attosecond pulse generation via the amplitude gating technique. The minimal pulse duration which can be obtained with this technique in argon without using dispersion elements is approximately 0.08–0.1 of the laser cycle for different intensities and frequencies of the fundamental. The cutoff regime is also characterized by a linear dependence of the harmonic phase on the fundamental intensity. The proportionality coefficient grows as the cube of the fundamental wavelength, thus this dependence becomes very important for the HHG by midinfrared fields. Moreover, for every high harmonic there is a *range* of laser intensities providing the generation in the cutoff regime and the atomic response magnitude in this regime can be greater than that in the plateau regime. Thus, the cutoff regime substantially contributes to the harmonic energy emitted under typical experimental conditions where the laser intensity varies in time and space.

DOI: 10.1103/PhysRevA.93.043416

I. INTRODUCTION

One of the most characteristic features of the high-order harmonic generation (HHG) by atoms, molecules, and ions in intense laser field is the plateau in the spectrum; namely, the region where the harmonic intensity almost does not depend on the harmonic order. The high-frequency part of the plateau ends up with a sharp decrease known as the cutoff of the harmonic spectrum [1–3]. The number of harmonics in the plateau increases with the fundamental intensity [3,4]. When the fundamental intensity increases the given harmonic first is generated at the cutoff and then within the plateau. At first glance, the former stage can be understood just as a sudden "turning on" of the generation, thus providing negligible contribution to the total signal. Using quantum-mechanical calculations we show that this is not the case. The cutoff regime can be attributed to a *range* of fundamental intensities and provides an important impact on the generation under typical experimental conditions. The dependence of the harmonic phase on the laser intensity substantially defines the phase-matching of the generation [5,6], spectral shift, and the harmonic line broadening [7–9], coherence [10], and the spatial properties of the harmonic beam [5,9,11,12]. Thus, the behavior of the harmonic phase in the cutoff regime has a pronounced effect on these properties. Moreover, the cutoff extreme ultraviolet (XUV) is used to generate an isolated attosecond pulse via the amplitude gating technique [13–17]. Studying the phase properties of these harmonics allows us to suggest the spectral range which should be used in this method to provide the shortest attosecond pulse for given pump intensity and frequency.

II. DEPENDENCE OF HARMONIC PHASE ON LASER INTENSITY

To analyze the HHG cutoff region theoretically we use a fully analytical result for the dipole moment [18] describing HHG emission by one electron bound to a zero-range potential in a monochromatic laser field. The dipole moment of the qth harmonic ($q = 2k + 1$) generated in the linearly polarized laser field $E(t) = E_0 \sin \omega t$ is presented in Ref. [18] as

$$d_{2k+1} = \frac{8}{\omega}\left(\pi \frac{U_p}{\omega} I_p\right)^{1/2} \frac{(-1)^k}{(2k+1)^2} \int_0^\infty \frac{d\tau}{\tau^{3/2}} e^{i(k+1/2)\tau} \times \{J_{k+1}[z(\tau)]\beta_+(\tau) \sin \alpha_{00k}(\tau) - J_k[z(\tau)]\beta_-(\tau) \cos \alpha_{00k}(\tau)\}, \quad (1)$$

where I_p is the ionization potential of the generating particle, $U_p = \frac{E_0^2}{4\omega^2}$ is the ponderomotive energy, τ is the electron excursion time, and the functions $z(\tau)$, $\beta_\pm(\tau)$, and $\alpha_{00k}(\tau)$ are defined as follows:

$$\beta_\pm(\tau) = \frac{e^{i\tau/2}}{1 \pm \frac{1}{2k+1}} - \frac{2}{\tau} \sin(\tau/2), \quad (2)$$

$$z(\tau) = \frac{U_p}{\omega}\left(\sin \tau - \frac{4 \sin^2(\tau/2)}{\tau}\right), \quad (3)$$

$$\alpha_{00k}(\tau) = \frac{I_p}{\omega}\tau + \frac{U_p}{\omega}\tau\left[1 - \left(\frac{\sin(\tau/2)}{\tau/2}\right)^2\right] - \frac{\pi}{4}(2k+1). \quad (4)$$

The dependence of the harmonic phase on the fundamental intensity was investigated in numerous studies: experimentally [19], numerically using the time-dependent Schrödinger equation (TDSE) solution [12,20], theoretically within the strong-field approximation [5,20,21,22], by using Feynman's path-integral approach [23] and the generalized semiclassical

*MargaritkaKhokhlova@gmail.com

model [24]. As was discussed in these works, the harmonic phase dependence can be described with the phase coefficient $\alpha_{2k+1} = -\frac{\partial \varphi_{2k+1}}{\partial I}$ where φ_{2k+1} is the phase of the spectral component d_{2k+1}. Considering the derivative of the dipole moment with respect to the laser intensity the phase coefficient α_{2k+1} can be found as

$$\alpha_{2k+1} = -\mathrm{Im}\left(\frac{1}{d_{2k+1}}\frac{\partial d_{2k+1}}{\partial I}\right). \tag{5}$$

Substituting Eq. (1) into Eq. (5), we derive the analytical equation for the phase coefficient α_{2k+1} in the form

$$\alpha_{2k+1} = \frac{1}{8\omega^3}\mathrm{Im}\left(\frac{\int_0^\infty \frac{d\tau}{\tau^{3/2}} e^{i(k+\frac{1}{2})\tau} D(\tau)}{\int_0^\infty \frac{d\tau}{\tau^{3/2}} e^{i(k+\frac{1}{2})\tau}[J_{k+1}(z)\beta_+ \sin\alpha_{00k} - J_k(z)\beta_- \cos\alpha_{00k}]}\right),$$

$$D(\tau) = \left(\sin\tau - \frac{4}{\tau}\sin^2(\tau/2)\right)\{[J_k(z) - J_{k+2}(z)]\beta_+ \sin\alpha_{00k} - [J_{k-1}(z) - J_{k+1}(z)]\beta_- \cos\alpha_{00k}\}$$

$$+ 2\tau\left[1 - \left(\frac{\sin(\tau/2)}{\tau/2}\right)^2\right][J_{k+1}(z)\beta_+ \cos\alpha_{00k} + J_k(z)\beta_- \sin\alpha_{00k}]. \tag{6}$$

In Fig. 1 we present the phase coefficient α_{17} calculated for H17 generated in Xe atoms by the laser field with the wavelength of 800 nm (below, the frequency of this field is denoted as $\omega_{\text{Ti:sapphire}}$). One can see that there are two different regimes for the behavior of the phase coefficient α with respect to intensity. The first regime (at lower intensities) corresponds to the cutoff region where the phase coefficient α is smooth, and the second regime (at higher intensities) corresponds to the plateau region where α behaves nonregularly. For the plateau region this can be explained by the quantum paths interference [25]. However, contributions of the long and short trajectories in the cutoff region cannot be well separated (and cannot even be accurately defined since the two saddle points in the action overlap). Therefore, the pronounced linear dependence of the harmonic phase in the cutoff region obtained without using the saddle-point approximation is a nontrivial result. Thus, we define the cutoff region as the one where α almost does not depend on the laser intensity (the criterion is that the value of α lays within $\pm 20\%$ of that for lowest intensity). The intensity corresponding to the change between these two regimes is denoted below as the cutoff-plateau transition intensity. Note, that as far as α oscillates with a large amplitude starting from the certain intensity (see Fig. 1), a different choice of the criterion would not change significantly the value of the cutoff-plateau transition intensity. Equation (6) for the phase coefficients can be simplified using the approximation for the end of the plateau and cutoff harmonics [see Eq. (5.23) in Ref. [18]]. These approximations allow to derive the following formula for the cutoff region:

$$\alpha \approx \frac{3.309}{4\omega^3}. \tag{7}$$

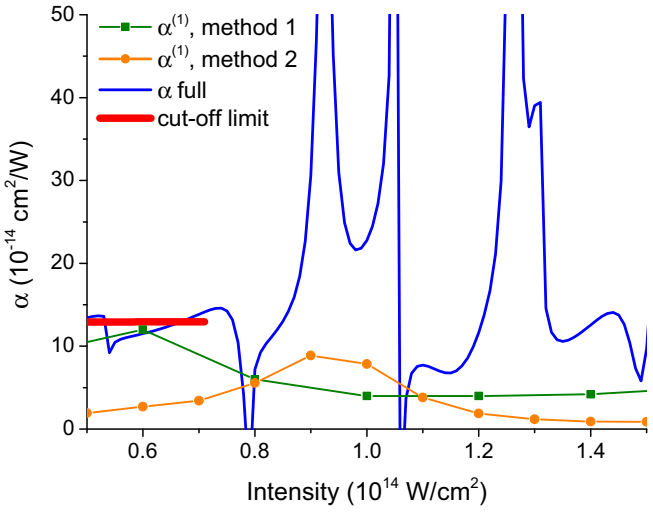

FIG. 1. The phase coefficient α for H17 generated in Xe as a function of laser intensity. The result obtained via Eq. (6) (blue line) and the approximation for the cutoff region (7) (thick red line) are presented. Lines with symbols show the results of two methods based on the numerical three-dimensional TDSE solution (the methods are described in the Appendix).

Note, that $\alpha \propto 1/\omega^3$ behavior can be illustrated by using following estimations: The harmonic phase φ is largely determined by the action S, which is the integral of the kinetic energy with respect to time (assuming that the potential energy is negligible for free electrons). Thus, $S \propto v^2\tau$, where $v \propto E_0/\omega$ is an electronic velocity, and $\tau \propto 1/\omega$ is an electronic excursion time. Therefore, $S \propto E_0^2/\omega^3$, where $E_0^2 \propto I$. Taking into account that $\alpha = -\partial\varphi/\partial I$ and $\varphi \propto S$ we find that the phase coefficient α is proportional to $1/\omega^3$. However, this estimation is obtained in terms of the quasiclassical trajectory (along which S is calculated) which is hardly accurate for the harmonics close to the cutoff as was discussed above. In spite of this, the estimation agrees with the strict analytical result given by Eq. (7).

Figure 1 shows that the approximation (7) agrees with the result of Eq. (6) in the cutoff region. Moreover, in the same figure we present results of α calculation by using two numerical methods discussed in detail in the Appendix. The methods are based on the numerical TDSE solution for a model one-electron atom with the technique described in Ref. [26]. The α values corresponding to the short trajectory only are presented in the plateau region (see lines with symbols in Fig. 1). We can see that the method 1 reasonably agrees with the analytical results but for the method 2 the agreement is

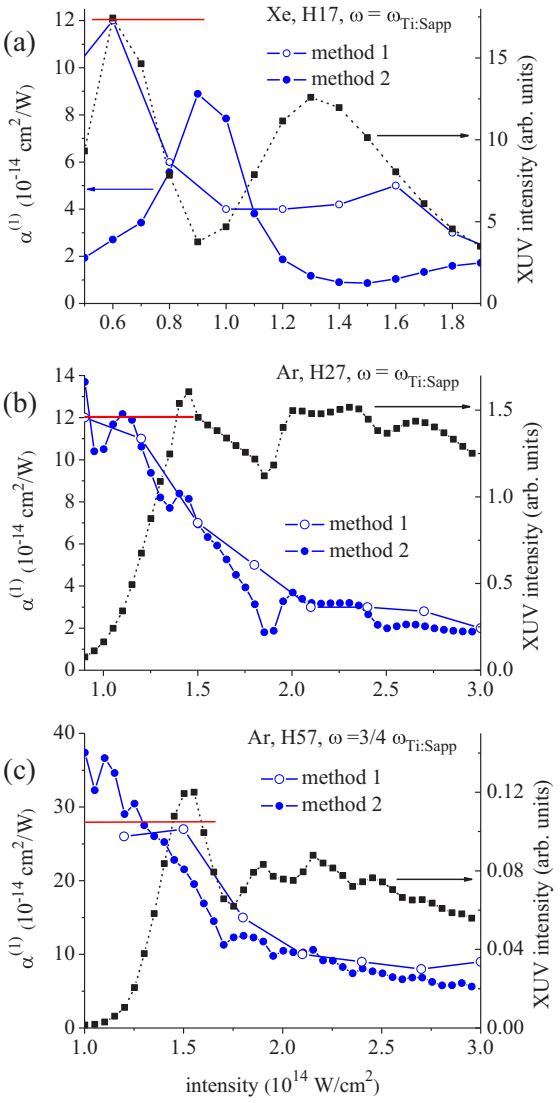

FIG. 2. $\alpha^{(1)}$ for the shortest trajectory contribution (solid blue) and the intensity (dotted black) of this contribution. The thick red line shows α for the cutoff harmonics given by Eq. (7). The results of method 1 (open circles) and method 2 (solid circles) calculated for H17 generated in Xe for (a) the laser wavelength 800 nm, (b) for H27 generated in Ar by the 800 nm laser field, and (c) for H57 generated in Ar by the 1067 nm laser field.

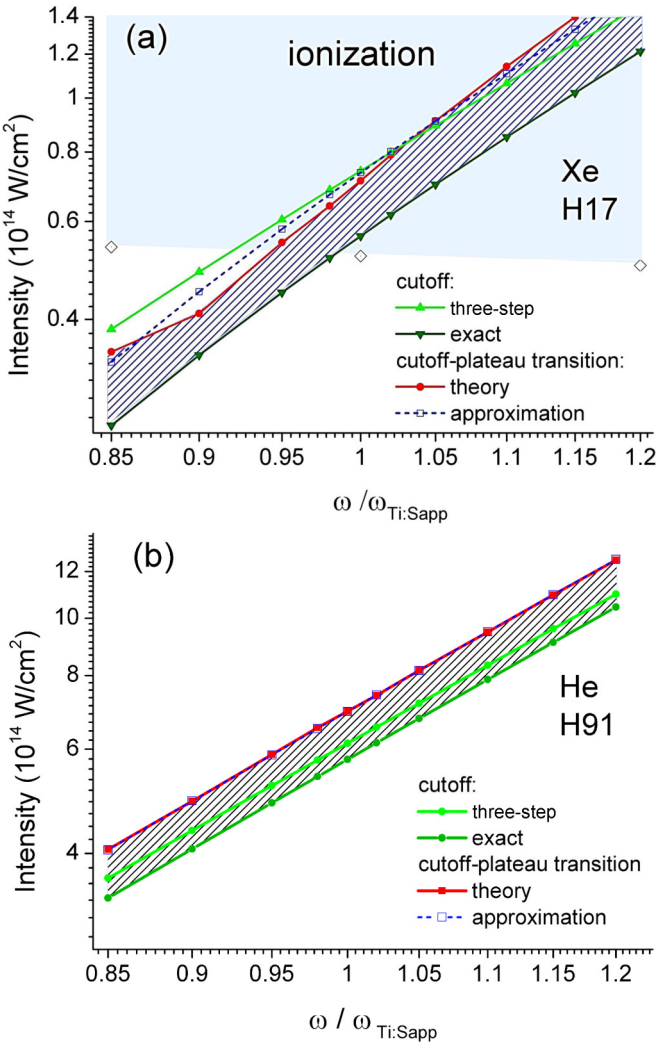

FIG. 3. The intensities corresponding to the cutoff-plateau transition obtained theoretically (red line) and approximately (blue dashed curve) for different fundamental frequencies. The three-step ("simple-man") and exact cutoff intensities (see text) are shown with light- and dark-green lines, respectively. The results are presented for (a) H17 generated by Xe atom and (b) H91 generated by He atom. The blue-filled area shows the region where the ionization is more than 10%.

worse. When the field parameters are closer to the tunneling regime both numerical methods agree with the analytical result [see Figs. 2(b) and 2(c)].

The numerically found values for α are lower than those for the long trajectory in the plateau regime but much higher than those for the short one. Thus, there is a significant difference between the cutoff and the plateau regime: in the latter there is at least the short trajectory contribution for which the phase dependence on the fundamental intensity can be neglected in many cases; for the cutoff regime this dependence is always considerable.

The cutoff-plateau transition intensity obtained by the criterion discussed above for the different fundamental frequencies is presented by the red curve in Fig. 3.

The areas below and above the red curve correspond to the cutoff and the plateau region, respectively. The green curves show the fundamental intensities at which the generation of the given harmonic starts: the light green curve shows this intensity found via the three-step-model (also called "simple-man") approach [27,28] and the dark-green one shows the result found by using the exact cutoff law [29]. Below we denote the exact cutoff intensity as I_{appear}. One can see that the cutoff-plateau transition can be approximated as $1.3I_{\text{appear}}$ (blue dashed curve) for the case of both H17 in Xe and H91 in He.

The generation takes place in the cutoff regime for the range of fundamental intensities shown by the hatched area between the red and dark-green curves in Fig. 3. With the numerical method described in the Appendix we calculate the intensity of the shortest trajectory contribution (equal to the full response in the cutoff regime and to the contribution of the short trajectory

in the plateau regime). In the cutoff regime this intensity achieves its maximum [see Fig. 2(b)] or it is close to the maximum [Figs. 2(a) and 2(c) and Fig. 8 in the Appendix]. Thus, in the experiments where the laser intensity generally varies in time and space, the contribution of the cutoff regime to the harmonic response is significant for many harmonics. Moreover, the laser intensity providing efficient HHG is practically limited by the medium ionization. Typically, several percent of the ionization provide an essential detuning from the phase matching [30]. This limitation practically cancels the HHG in the plateau regime for certain harmonics. To illustrate this we find by using the numerical TDSE solution the intensities leading to more than 10% ionization of Xe atoms by 15 fs laser pulse. As presented in Fig. 3(a), H17 is generated in Xe in the cutoff regime *only* for laser frequencies higher than approximately $0.95\omega_{\text{Ti:sapphire}}$. The intensities providing similar ionization for helium are higher than those shown in Fig. 3(b), so in this case the generation of H91 can take place in both regimes.

Note, that the sensitivity of the harmonic phase on the laser intensity influences many HHG features such as phase matching, divergence, etc. The rapid increase of α with laser wavelength makes this sensitivity even more important for HHG in few-micron laser fields, which recently have been actively used to generate very high harmonic orders; see Refs. [31,32] and others.

III. DEPHASING OF CUTOFF HARMONICS

The second part of our study deals with the dephasing between successive harmonics. The phase locking of the harmonics makes it possible to generate attosecond pulses. The cutoff region is especially important for the so-called amplitude gating method of an isolated attosecond pulse generation: the cutoff XUV is generated by a few-cycle laser pulse during one half cycle only in the maximum of the laser pulse for the certain carrier envelope phase [13–17].

Using the numerical three-dimensional (3D) TDSE solution for a model argon atom [33] we investigate the duration of the attosecond pulse from cutoff harmonics as a function of its spectral width and the fundamental frequency. In Fig. 4 we present the attosecond pulses generated by using different numbers of harmonics. We start from the case when the attosecond pulse is obtained by using all the harmonics above the cutoff one including it, and then we add the adjacent lower harmonics one by one. In Fig. 4 one can see that, initially, the increasing number of harmonics leads to the decrease of the attosecond pulse duration. This is explained by the equal dephasing between successive harmonics which results in the same emission time t_e ($t_e = \frac{\partial\varphi}{\partial\omega} = \frac{\Delta\varphi}{2\omega}$ where $\Delta\varphi$ is the dephasing, or the spectral phase difference, between two consecutive harmonics [34,35]), thus the decrease of the attopulse duration is a manifestation of the uncertainty principle. However, adding lower harmonics with emission time differing from that of the cutoff harmonics leads to the increase of the attopulse duration (see red dotted curves in Fig. 4) and generation of two or more attosecond pulses. These pulses can be attributed to the short- and long-trajectory contributions in the plateau region [35]. Below we denote q_{low} corresponding to the shortest attosecond pulse duration as $q_{\text{low}}^{\text{opt}}$

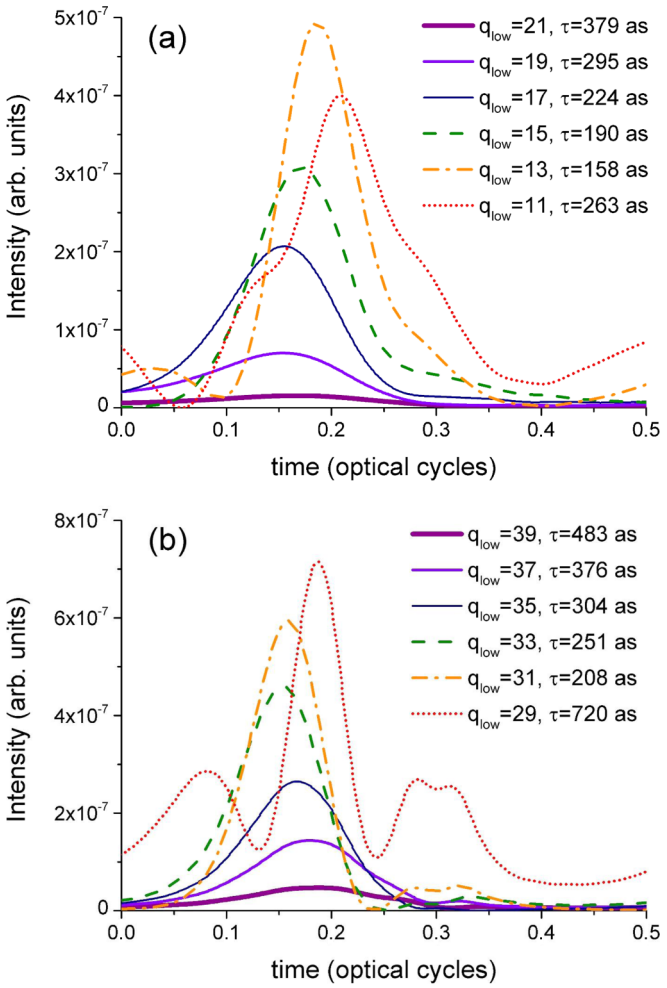

FIG. 4. Calculated attosecond pulses obtained by using all harmonics higher than q_{low} shown in the legends. (a) Laser frequency is $1.5\omega_{\text{Ti:sapphire}}$ and intensity 4.6×10^{14} W/cm^2, corresponding to cutoff at the 21st harmonic. (b) Laser frequency is $\omega_{\text{Ti:sapphire}}$ and intensity 2.4×10^{14} W/cm^2, corresponding to the cutoff at the 39th harmonic.

and introduce the parameter $\beta = \frac{q_{\text{cutoff}} - q_{\text{low}}^{\text{opt}} + 1}{q_{\text{cutoff}}}$ characterizing the ratio of the number of harmonics minimizing the attopulse duration to the total number of generated harmonics. For the conditions of Fig. 4(a) we find $\beta = 0.43$ and for those of Fig. 4(b), $\beta = 0.23$.

In Fig. 5, the values for β are shown for different intensities and frequencies of the laser field. These are chosen as follows: first we calculate the spectrum for the laser field with wavelength of 800 nm and intensities corresponding to the three-step cutoff frequency at 27H, 33H, and 39H. The energies of the cutoff harmonics are 41.9, 51.2, and 60.5 eV, respectively. Besides, we consider other laser frequencies and intensities such that the cutoff takes place at these energies.

One can see that the parameter β (solid lines in Fig. 5) increases with increasing fundamental frequency while the corresponding attosecond pulse shortens. The shortest attopulse duration obtained in our calculations is less than 150 as. Moreover, as the generation conditions get closer to the tunneling regime the β parameter decreases. At the same time,

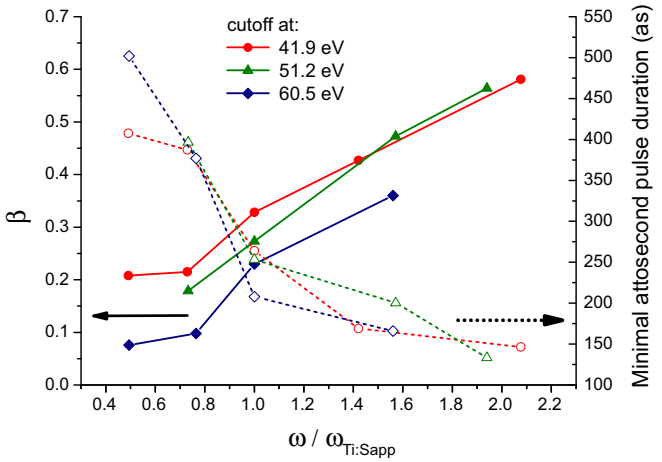

FIG. 5. Parameter β (solid lines) and the single-attosecond-pulse duration (dashed lines) for certain values of β for different laser intensities corresponding to 41.9 eV (red), 51.2 eV (green), and 60.5 eV (blue) cutoff harmonic energies.

the minimal attosecond pulse duration *for the given frequency* almost does not depend on the fundamental intensity. The shortest attosecond pulse duration is 0.08–0.1 of the laser cycle for different intensities and frequencies of the fundamental. For the frequency of the Ti:sapphire laser this agrees very well with the experimentally found duration of 250 as [17].

IV. CONCLUSION

We find that the cutoff regime can be defined as the regime having regular linear dependence of the harmonic phase on the fundamental intensity. The phase coefficient in the cutoff regime is well approximated by Eq. (7). The phase coefficient grows as the cube of the fundamental wavelength; therefore, this dependence becomes very important for the HHG by midinfrared fields. The value of the phase coefficient is much higher than that for the short trajectory in the plateau regime. We show that HHG takes place in the cutoff regime for a *range* of intensities and that the XUV intensity within this range is comparable or even higher than in the plateau regime. This makes the studies of the cutoff regime rather important from the practical viewpoint. Moreover, for rather high harmonics the generation occurs mainly within this range because the medium ionization practically limits the fundamental intensity for which the HHG takes place.

The change of the harmonic phase locking when HHG evolves from the cutoff to the plateau regime determines the optimal bandwidth of the spectral region that should be used for the attosecond pulse production via the amplitude gating technique. We find that the minimal pulse duration that can be obtained with this technique using argon as generating medium without utilizing dispersion elements is approximately 0.08–0.1 of the laser cycle; this result is found for different laser intensities and for frequencies of the fundamental from $0.5\omega_{\text{Ti:sapphire}}$ to $2\omega_{\text{Ti:sapphire}}$. Using filters with the proper dispersion [36] or chirped multilayer mirrors [37] is necessary to obtain shorter attosecond pulses.

ACKNOWLEDGMENTS

This study was supported by RFBR (Grant No. 16-02-00858) and by RSF (Grant No. 16-12-10279).

APPENDIX

We solve numerically the one-electron 3D TDSE for a model Xe atom in the laser field. The numerical method is described in Ref. [26]. The soft Coulomb potential providing the ionization energy equal to the Xe ionization energy is used. We reconstruct the α values from the TDSE solution as discussed below.

Method 1 is a development of the method suggested in Refs. [20,38] where α was reconstructed from the spectra emitted under different peak intensities of the Gaussian laser pulse. However, we use very a specific temporal envelope (see Fig. 6) of the laser intensity: the intensity rapidly increases at the leading edge of the pulse during time τ_f, then it slowly and *linearly* grows during time τ, and finally it decreases during time τ_f. The intensity is given as

$$I(t) = I_0 f(t)\left(1 + \gamma \frac{\omega t}{2\pi}\right), \tag{A1}$$

where

$$f(t) = \begin{cases} -\tau/2 - \tau_f < t < -\tau/2, & \sin^2\left(\frac{t+\tau/2+\tau_f}{\tau_f}\frac{\pi}{2}\right) \\ -\tau/2 < t < \tau/2, & 1 \\ \tau/2 < t < \tau/2 + \tau_f, & \sin^2\left(\frac{t-[\tau/2+\tau_f]}{\tau_f}\frac{\pi}{2}\right). \end{cases} \tag{A2}$$

The harmonics are emitted mainly in the region of the linear growth of the intensity. The linear dependence of the harmonic phase on the laser intensity is transmitted in the linear dependence of the phase on time, thus in the harmonic frequency shift. The presence of several contributions to HHG leads to the line splitting, as shown in Fig. 7. The value of α

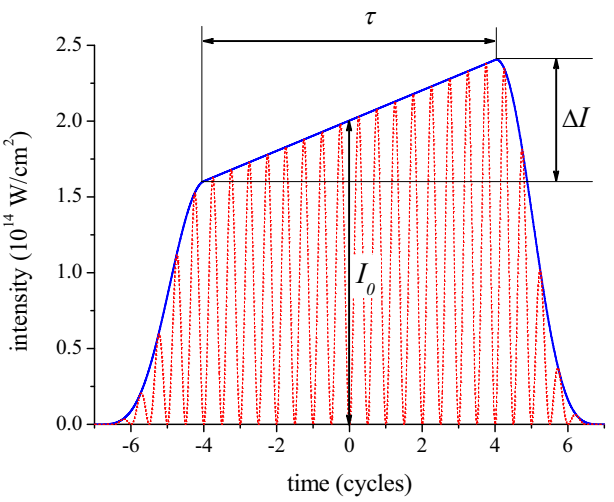

FIG. 6. Laser pulse intensity (solid blue line) given by Eq. (A1). After $\tau_f = 3$ cycles turning on, the intensity increases linearly during $\tau = 8$ cycles, and then turns off during 3 cycles. Dotted red line presents the square of the field.

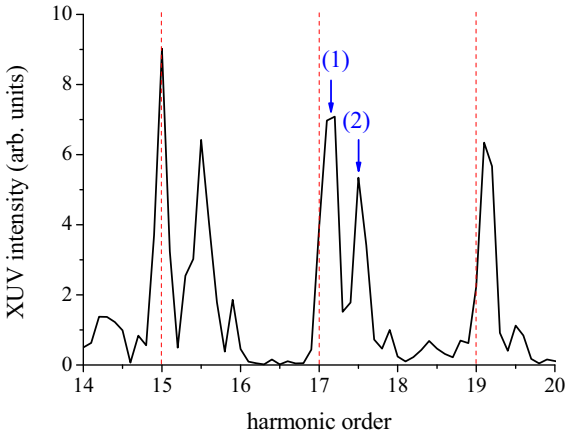

FIG. 7. Harmonic spectrum found via numerical three-dimensional TDSE solution for the model Xe atom. The laser wavelength is 800 nm and the laser intensity envelope is shown in Fig. 6. Red dashed lines show exact harmonic frequencies. One can see the shortest trajectory contribution (1), next-to-shortest trajectory contribution (2), and the contributions from other trajectories.

for every contribution can be reconstructed from the frequency shift of every peak (as well as the weight of the contribution can be reconstructed from the weight of the peak). Namely, the spectral component with the frequency shift $\delta\omega$ corresponds to

$$\alpha = 2\pi \frac{\delta\omega}{\omega} \frac{1}{\gamma I_0}. \tag{A3}$$

The accuracy of the method is limited by the following: using too short τ leads to the wide spectral peaks (due to the uncertainty principle), and using too long τ provides full ionization and high variation of the intensity within the pulse ΔI, so it is unclear which laser intensity corresponds to the found α. In general, this method is effective for the contributions with high α: even slow intensity growth leads to the pronounced shift of the spectral peak.

In Fig. 8 we compare α maps found for different τ and γ. One can see that the features of the maps are rather sensitive to these parameters. Certainly, this is not a drawback of the method but a manifestation of the uncertainty principle. The main properties are similar for all the maps presented: when the harmonic is generated in the cutoff regime it is rather intense and α is about ten. For higher intensities there are several contributions with different values of α. In particular, in the lower right panel (having the best resolution in terms of α and, thus, the worst resolution in terms of intensity) we can clearly see the two contributions corresponding to the short ($\alpha \approx 3$) and long ($\alpha \approx 20$) trajectories for the electronic excursion time less then one cycle and (surprisingly intense) contribution from the trajectory with longer excursion time ($\alpha \approx 45$).

Method 2 is based on the TDSE numerical solution in which contributions of all trajectories except the shortest one are artificially suppressed. The technique of this suppression was described in Ref. [39]. In this method specific shape of the the laser pulse is not important. We use the intensity given by

$$I(t) = I_0 f(t), \tag{A4}$$

where $f(t)$ is given by Eq. (A2), τ_f is three laser cycles, and τ is four cycles.

From the harmonic phase $\varphi^{(1)}(I_0)$ [the index (1) shows that only the shortest trajectory contribution is taken into account in this method] calculated for different I_0 we then find $\alpha^{(1)} = -\partial\varphi^{(1)}/\partial I_0$, see Fig. 2. The harmonic intensity found in these calculations gives the intensity of the "shortest" trajectory contribution as the function of the laser intensity. This contribution corresponds to the full response in the cutoff regime and the contribution of the short trajectory in the plateau regime.

Comparison of the methods is presented in Fig. 2. To find $\alpha^{(1)}$ with method 1 we choose the peak corresponding

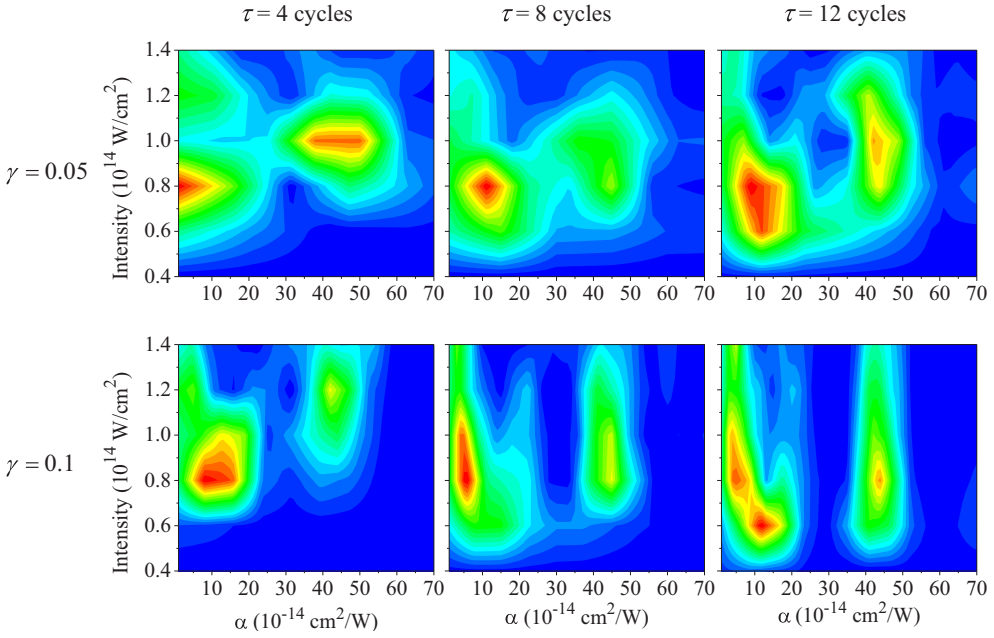

FIG. 8. α maps calculated for different τ and γ for H17 in Xe. The laser wavelength is 800 nm.

to the lowest value of α for every intensity. The results of both methods are very close to each other in the tunneling regime [Figs. 2(b) and 2(c)] and are less close for conditions intermediate between tunneling and multiphoton regimes [Fig. 2(a)]. Method 2 is less reliable in these conditions because the quantum trajectory separation used in this method is hardly applicable. However, in all three cases for the harmonic generated in the cutoff regime, method 1 gives a value of α that is close to the theoretical estimation given by Eq. (7).

[1] A. McPherson, G. Gibson, H. Jara, U. Johann, T. S. Luk, I. A. McIntyre, K. Boyer, and C. K. Rhodes, J. Opt. Soc. Am. B **4**, 595 (1987).

[2] M Ferray, A. L'Huillier, X. F. Li, L. A. Lompre, G. Mainfray, and C. Manus, J. Phys. B: At., Mol. Opt. Phys. **21**, L31 (1988).

[3] X. F. Li, A. L'Huillier, M. Ferray, L. A. Lompré, and G. Mainfray, Phys. Rev. A **39**, 5751 (1989).

[4] J. L. Krause, K. J. Schafer, and K. C. Kulander, Phys. Rev. Lett. **68**, 3535 (1992).

[5] M. Lewenstein, P. Salieres, and A. L'Huillier, Phys. Rev. A **52**, 4747 (1995).

[6] J. Peatross, M. V. Fedorov, and K. C. Kulander, J. Opt. Soc. Am. B **12**, 863 (1995).

[7] J. Zhou, J. Peatross, M. M. Murnane, H. C. Kapteyn, and I. P. Christov, Phys. Rev. Lett. **76**, 752 (1996).

[8] V. T. Platonenko, V. V. Strelkov, G. Ferrante, V. Miceli, and E. Fiordilino, Laser Phys. **6**, 1164 (1996).

[9] A. Dubrouil, O. Hort, F. Catoire, D. Descamps, S. Petit, E. Mevel, V. V. Strelkov, and E. Constant, Nat. Commun. **5**, 4637 (2014).

[10] M. Bellini, C. Lynga, A. Tozzi, M. B. Gaarde, T. W. Hansch, A. L'Huillier, and C.-G. Wahlstrom, Phys. Rev. Lett. **81**, 297 (1998).

[11] J. Peatross and D. D. Meyerhofer, Phys. Rev. A **51**, R906(R) (1995).

[12] M. B. Gaarde, F. Salin, E. Constant, Ph. Balcou, K. J. Schafer, K. C. Kulander, and A. L'Huillier, Phys. Rev. A **59**, 1367 (1999).

[13] I. P. Christov, M. M. Murnane, and H. C. Kapteyn, Phys. Rev. Lett. **78**, 1251 (1997).

[14] V. T. Platonenko and V. V. Strelkov, Quantum Electron. **28**, 564 (1998).

[15] G. G. Paulus, F. Grasbon, H. Walther, P. Villoresi, M. Nisoli, S. Stagira, E. Priori, and S. De Silvestri, Nature (London) **414**, 182 (2001).

[16] M. Hentschel, R. Kienberger, Ch. Spielmann, G. A. Reider, N. Milosevic, T. Brabec, P. Corkum, U. Heinzmann, M. Drescher, and F. Krausz, Nature (London) **414**, 509 (2001).

[17] R. Kienberger, E. Goulielmakis, M. Uiberacker, A. Baltuska, V. Yakovlev, F. Bammer, A. Scrinzi, Th. Westerwalbesloh, U. Kleineberg, U. Heinzmann, M. Drescher, and F. Krausz, Nature (London) **427**, 817 (2004).

[18] W. Becker, S. Long, and J. K. McIver, Phys. Rev. A **50**, 1540 (1994).

[19] D. C. Yost, T. R. Schibli, J. Ye, J. L. Tate, J. Hostetter, M. B. Gaarde, and K. J. Schafer, Nat. Phys. **5**, 815 (2009).

[20] M. B. Gaarde and K. J. Schafer, Phys. Rev. A **65**, 031406 (2002).

[21] Ph. Balcou, A. S. Dederichs, M. B. Gaarde, and A. L'Huillier, J. Phys. B: At., Mol. Opt. Phys. **32**, 2973 (1999).

[22] Ph. Antoine, A. L'Huillier, M. Lewenstein, P. Salieres, and Bertrand Carre, Phys. Rev. A **53**, 1725 (1996).

[23] P. Salieres, B. Carre, L. Le Deroff, F. Grasbon, G. G. Paulus, H. Walther, R. Kopold, W. Becker, D. B. Milosevic, A. Sanpera, and M. Lewenstein, Science **292**, 902 (2001).

[24] J. A. Hostetter, J. L. Tate, K. J. Schafer, and M. B. Gaarde, Phys. Rev. A **82**, 023401 (2010).

[25] A. Zair, M. Holler, A. Guandalini, F. Schapper, J. Biegert, L. Gallmann, U. Keller, A. S. Wyatt, A. Monmayrant, I. A. Walmsley, E. Cormier, T. Auguste, J. P. Caumes, and P. Salieres, Phys. Rev. Lett. **100**, 143902 (2008).

[26] V. V. Strelkov, A. F. Sterjantov, N. Yu. Shubin, and V. T. Platonenko, J. Phys. B: At., Mol. Opt. Phys. **39**, 577 (2006).

[27] P. B. Corkum, Phys. Rev. Lett. **71**, 1994 (1993).

[28] K. J. Schafer, B. Yang, L. F. DiMauro, and K. C. Kulander, Phys. Rev. Lett. **70**, 1599 (1993).

[29] M. Lewenstein, Ph. Balcou, M. Yu. Ivanov, A. L'Huillier, and P. B. Corkum, Phys. Rev. A **49**, 2117 (1994).

[30] S. Kazamias, S. Daboussi, O. Guilbaud, K. Cassou, D. Ros, B. Cros, and G. Maynard, Phys. Rev. A **83**, 063405 (2011).

[31] B. Sheehy, J. D. D. Martin, L. F. DiMauro, P. Agostini, K. J. Schafer, M. B. Gaarde, and K. C. Kulander, Phys. Rev. Lett. **83**, 5270 (1999).

[32] B. Shan and Z. Chang, Phys. Rev. A **65**, 011804(R) (2001).

[33] V. V. Strelkov, V. T. Platonenko, and A. Becker, Phys. Rev. A **71**, 053808 (2005).

[34] Y. Mairesse, A. de Bohan, L. J. Frasinski, H. Merdji, L. C. Dinu, P. Monchicourt, P. Breger, M. Kovacev, R. Taieb, B. Carre, H. G. Muller, P. Agostini, and P. Salieres, Science **302**, 1540 (2003).

[35] K. Varju, Y. Mairesse, B. Carre, M. B. Gaarde, P. Johnsson, S. Kazamias, R. Lopez-Martens, J. Mauritsson, K. J. Schafer, Ph. Balcou, A. L'Huillier, and P. Salieres, J. Mod. Opt. **52**, 379 (2005).

[36] R. Lopez-Martens, K. Varju, P. Johnsson, J. Mauritsson, Y. Mairesse, P. Salieres, M. B. Gaarde, K. J. Schafer, A. Persson, S. Svanberg, C.-G. Wahlstrom, and A. L'Huillier, Phys. Rev. Lett. **94**, 033001 (2005).

[37] E. Goulielmakis, M. Schultze, M. Hofstetter, V. S. Yakovlev, J. Gagnon, M. Uiberacker, A. L. Aquila, E. M. Gullikson, D. T. Attwood, R. Kienberger, F. Krausz, and U. Kleineberg, Science **320**, 1614 (2008).

[38] P. Balcou, P. Salieres, A. L'Huillier, and M. Lewenstein, Phys. Rev. A **55**, 3204 (1997).

[39] V. V. Strelkov, A. A. Gonoskov, I. A. Gonoskov, and M. Yu. Ryabikin, Phys. Rev. Lett. **107**, 043902 (2011).